ICSV 21
13-17 July, 2014, Beijing/China

The 21st International Congress on Sound and Vibration

13-17 July, 2014, Beijing/China

MODELLING OF THE DYNAMIC INTERACTION BETWEEN A REACTING SPRAY AND AN ACOUSTIC FIELD IN A TURBULENT COMBUSTOR

Virginia Fratalocchi, Jim B. W. Kok

Laboratory of Thermal Engineering, Faculty of Engineering Technology, University of Twente, Enschede, The Netherlands

e-mail: v.fratalocchi@utwente.nl

The work presented in this paper is a first attempt at tracing both the vaporization droplet history and the momentum exchange between the liquid and gas phase, in a reacting flow field exposed to acoustic propagation waves. The liquid phase is tracked with a Lagrangian approach, while the carrier gas phase is modelled in an Eulerian framework, based in a two-way coupling interaction, under the main assumptions of dilute regime and infinite thermal conductivity. Acoustic propagating waves will eventually affect the combustion dynamic due to oscillating heat released by the flame. Aim of this work is to assess a strategy to estimate the effect of an oscillating gas velocity field on: droplet displacement, redistribution of the characteristic droplet diameters, changes in the evaporation rate. Assuming the hypothesis of dilute regime as valid, the study is carried out by means of a non-dimensional number characterization.

1. Introduction

The dynamic interaction between droplets in a spray and the velocity fluctuations induced by an acoustic field is important to study with a view to thermo acoustic oscillations. Spray flame instabilities have been the object of several numerical and experimental investigations aimed at gaining insight into the physical phenomena that characterize the flame response at thermoacoustic oscillations. Modelling of reacting sprays is a difficult task due to the interaction of several phenomena, occurring at different temporal and spatial scales, such as atomization, droplet collisions, heating and evaporating droplets, heat and mass inter-phase transfers, as well as momentum changes and chemistry. Efforts have been described in literature to study the droplet lifetime, the role played by the liquid phase in the gas phase turbulence field, and the different approaches that have been used in the combustion modelling. If the turbulence is most likely acting on the aerodynamic interaction between the two phases, and on the droplet displacement, an oscillating gas velocity field will also affect the evaporation rate. In case of a chemically reacting spray the situation is even more challenging due to the oscillating heat released by the flame.

2. Test case

The original piloted spray burner has been developed at University of Sydney[1]. A detailed description of the geometry and a wide set of initial conditions adopted in experimental set-up of non-reacting jets and flames can be found elsewhere[1,2]. The flame, burning at atmospheric pressure in a non–confined environment, is stabilized by a pilot flame, surrounded itself by a laminar stream of co-flow air. A schematic of the burner is shown in Fig. 2.1 (a), where the blue dashed line corresponds to the nozzle exit plane. The nozzle diameter is 10,5 mm, and the pilot annulus has a diameter of 25 mm. The pilot flame holder is located 7 mm upstream of the nozzle exit. The nebulizer is centred inside the burner and phenomena of break-up and droplets collisions do not affect the flow field at the nozzle exit. The design of the burner allows for the main assumption of presuming the spray in the dilute regime. Break-up, collisions and agglomeration phenomena take place along the pipe, so that at the nozzle exit plane the volume occupied by the liquid phase is small compared to the gas phase, and no droplet interactions are numerically modelled. The injection physics are taken into account by means of droplet sizes and velocities as boundary conditions. Five discrete droplet size groups are defined by the value of the mean diameter. The $15\mu m$ drop diameter is representative of the 10-20 μm size class, and so on, with the bigger tracked particle of $45\mu m$. The mass fraction assigned to each class is in respect of the experimental data, although the sample size is insufficiently large due to the high computational cost. Condition of zero slip velocity is forced at the jet nozzle, but a not uniform velocity magnitude is defined along the radial direction, according to the experimental data. The droplets injection occurs at specified time steps, over a total simulation time equal to $0.1s$, and a numeric time step of the order of $2.0e-6\ s$. The computational domain is discretised with a structured mesh of $10e6$ nodes, and the minimum size cell, located at the nozzle exit, is of $0.5\ mm$. RANS simulations have been run first, to test the quality of the grid and the minimum value of the slice angle to be used, which is of 20^o. A detail of the grid is provided in Fig. 2.1 (c), where the x-z plane is the inlet plane, corresponding to the nozzle exit plane of the real burner.

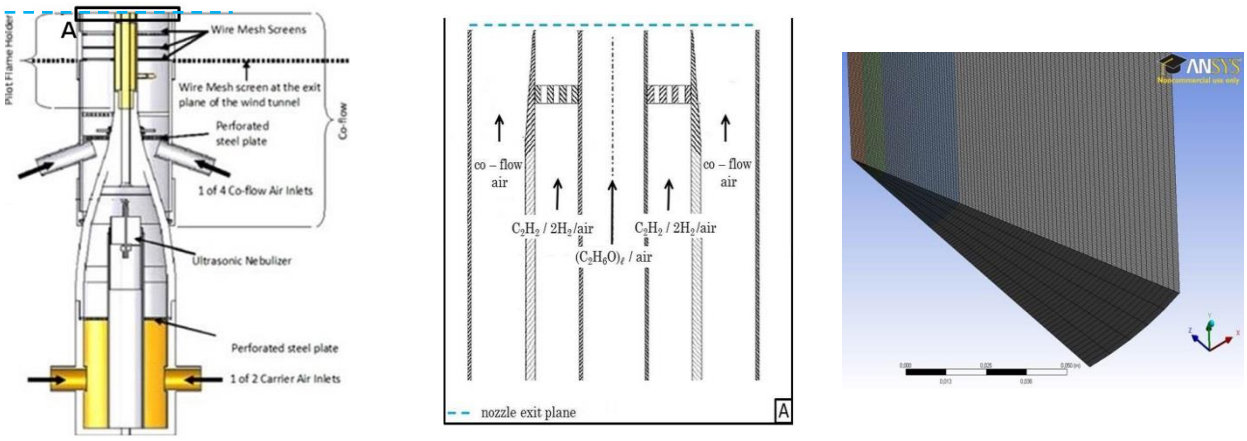

(a) (b) (c)

Figure 2.1. Schematic of the spray burner[1] (a), detail of the nozzle at the exit plane (–) (b), detail of the computational grid domain (c),

3. Numerical simulation

The CFD analysis is carried out with a commercial numerical code, CFX. The Eulerian-Lagrangian approach is used, where the gas phase properties are solved in the domain and after interpolated at the particle locations, by a tri-linear interpolation. In this section the numerical ap-

proach is briefly described, but a more detailed overview of the numerical model of reacting multiphase flow can be found elsewhere[3,4].

The momentum exchange is governed by the drag law defined with the Schiller-Neumann model[5]. The transport equation for the particle temperature, T_P, results from the contributions of the radiative and convective heat transfer, and the term due to the evaporation. Assuming the radiative heat transfer negligible, and the Lewis number equal to one, the transport equation of the droplet temperature is:

$$m_P c_P \frac{dT_P}{dt} = \pi d_P k Nu (T_g - T_P) \zeta \left(\frac{1}{e^{\zeta} - 1} \right) + \dot{m}_P \Delta h_{vap} \tag{1}$$

where T_g is the gas phase temperature and the subscript "p" refers to the dispersed phase. The Nusselt number, Nu, is formulated with the Ranz and Marshall[6] correlation:

$$Nu = 2 + 0.6\, Re_p^{1/2} Pr^{1/3} \tag{2}$$

The ζ factor, in Eq. (1), is defined as follows:

$$\zeta = \frac{c_{pg} |\dot{m}_P|}{\pi d k_g Nu} \tag{3}$$

when multiphase reactions are involved, the heat transfer due to convection is corrected by a blowing factor, Eq. (3), based on the rate of mass transfer. One can also look at this factor as a modified Nu number which takes into account the instantaneous mass and heat transfer. Δh_{vap} is the latent heat of vaporization. Moreover, the particle temperature is assumed to be spatially uniform within the droplet, and equilibrium conditions to prevail at the surface.

The liquid evaporation rate is modelled as follows[3]:

$$\frac{dm_P}{dt} = \pi d_P \varrho D \frac{W_{vap}}{W_{mix}} ln \left(\frac{1 - X_s^v}{1 - X_{vap}^v} \right) Sh \tag{4}$$

with the Sherwood number modelled in analogy with Nu number. X_s^v is the equilibrium vapour mole fraction of the evaporating component at the droplet surface, X_{vap}^v is the mole fraction of the evaporating component in the gas phase, ϱD is the dynamic diffusivity of the component in the continuum and $W_{vap,mix}$ are respectively the molecular weights of the vapour and the mixture, in the continuous phase. The URANS set of equations is used to model the gas phase, where the two-way coupling with the liquid phase is ensured by the inclusion of the source terms. The pilot flame is modelled as hot exhaust gas, of a stoichiometric mixture of acetylene / hydrogen / air. In this work, chemical reaction is modelled with a single step reaction mechanism. The combustion is treated with the combined EDM/Finite Rate Chemistry Model, and the controlling reaction rate is given by the minimum between the computed mixing time scale and the chemical reaction rate.

4. Thermo-acoustic analysis

The characterization of the spray flame response to acoustic forcing covers a wide range of phenomena involving different temporal scales. As previously mentioned, in the present test case, the flow field is not affected by droplets interactions. This leads to the simplifying assumption that oscillatory deformations and break up do not take place under the spray-acoustic interaction. The particles keep the spherical shape and the dilute regime is preserved. The analysis of the spray-

acoustics interaction can be described looking at four characteristic times. The acoustic time, corresponding to the forcing frequency $(1/f_f)$, and the time scales associated with the turbulence, the heat and mass transfer, so that the evaporation, and the inter-phase momentum exchanges. The turbulent eddy frequency will be discussed in the next section, in relation with the chemical reaction rate. To evaluate the regimes of droplet response in a reacting oscillating environment, the magnitude of the droplet lifetime and the relaxation time are taken into account. Estimation of the response of the particle to a perturbation in the flow is made under the simplifying case of Stokes flow:

$$\tau_P = \frac{\rho_l d^2}{18\mu_g} \tag{5}$$

The droplet lifetime, as modelled in CFX, is given by:

$$\tau_{evap} = d_0^2 \Big/ \left[8 \frac{\rho_s}{\rho_l} D_s \frac{W_{vap}}{W_{mix}} ln\left(\frac{1 - X_s^v}{1 - X_{vap}^v} \right) Sh \right] \tag{6}$$

For a given droplet size class, the condition $t_{evap} > \tau_{acoustic}$ determines whether or not the particle will survive at the entire acoustic cycle before to evaporate, and so corresponds to the lower limit for the cut-off forcing frequency. Theoretically, when $t_{evap} > \tau_P$, two distinctive droplet regimes response may be distinguished. At low frequency, the spray response characterised by a solely evaporation rate changes, and at high frequency by dispersion involving both thermodynamics and mechanical effects. When $t_{evap} = \tau_P$ both phenomena of momentum and evaporation changes are expected to take place. From the calculated reacting flow field, $\tau_p/\tau_{evap} \approx 0.65$ which means that the thermodynamics and the aerodynamics features of the liquid phase may have the same influence on the forced flame response. Nevertheless, the dynamics cannot be stated a priori, since the evaporation rate, not only depends on the droplet size, but also on the location within the domain. An estimation of the cut-off forcing frequency is based on the transient case results, and it is around $140\ Hz$, for the medium size droplets.

5. Results

Figure 5.1 (a) and (b) show the contours of the instantaneous temperature flow field obtained in the transient calculation run, and the fuel vapour mass fraction at $t = 20ms$. It is clear that the combustion starts at the edge of the spray, where the fuel vapour enters the hot exhaust gases, while the core of the flame is a cold region. The mixing, towards the pilot, enhances the reaction rate, which develops faster in the axial direction. Fig. 5.1(c) is a detail of the core of the spray, where the diameter distribution of the droplets is shown, over the temperature gas phase field. When the temperature is getting higher, the droplet diameter decrease, and only few droplets overcome the burning region without evaporating. Explanation for that can also be found in the slip velocity profile. Across the evaporation zone, towards the burning region, the value of the slip velocity reverse to positive values, in particular for bigger size classes. As observed also in experimental set-up[1,2], due to their bigger relaxation time, the bigger droplets tend to keep their velocities even after a deceleration of the gas phase. Nevertheless, in this work, liquid turbulent dispersion is not taken into account, and so the liquid deceleration, and their momentum dissipation, is expected to be underpredicted. The radial heat and mass transfer, and so the fuel vapour formation is also affected by this simplification, and under-estimated.

The flame length, evaluated with the maximum temperature, is about $10cm$ overpredicted, and this can be explained looking at the combustion model. According to the experimental data, the

temperature along the centreline should increase closely to the nozzle. In Fig. 5.1 the core zone is visibly at cold temperature, and the ethanol fuel reaches the saturation temperature between $y/D = 10$ and $y/D = 15$, where y is the axial direction and D the nozzle diameter. The heat and mass transfers are reaction rate controlling, through the local mixture concentration of fuel and air, which determines the chemical reactions. The initial reaction time scale might be under-predicted, and the mixing is not high enough to enhance the heat transfer from the edge to the core of the spray, and thus to trigger the combustion closely to the nozzle. The evaporation time associated to the smaller scale in the reacting field is of the order of ms, at least one order of magnitude bigger than the turbulent time scale, as can be seen in Fig. 5.2.

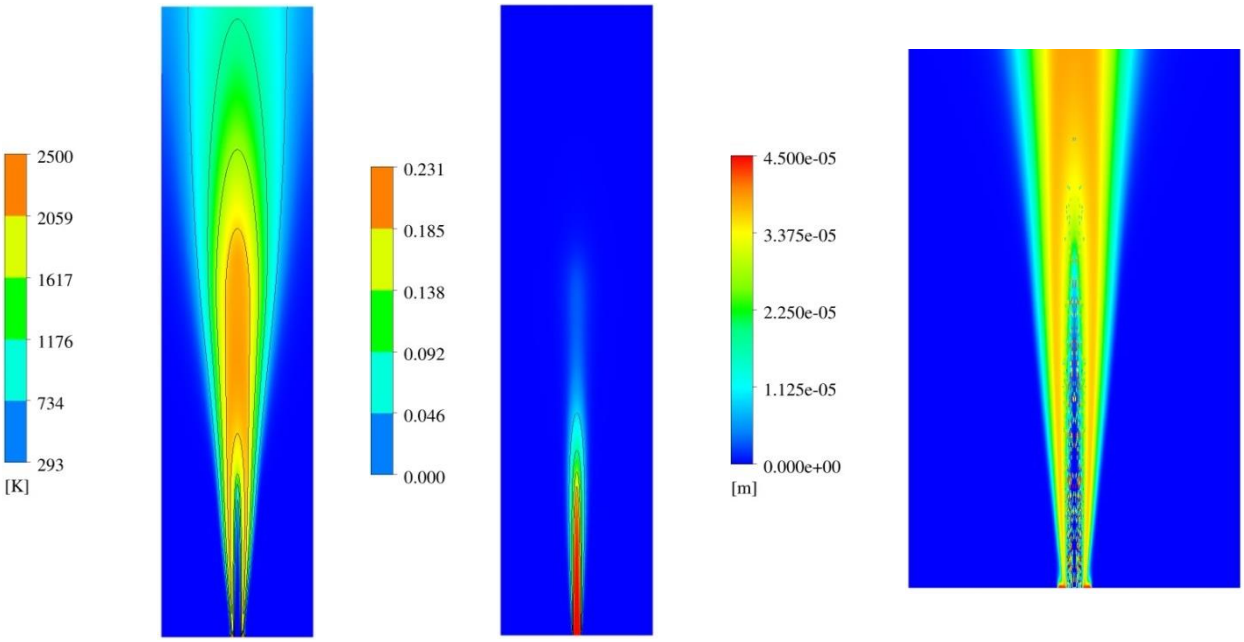

Figure 5.1. Instantaneous temperature (a), C_2H_6O mass fraction (b), liquid droplets diameter (c), at t=20ms.

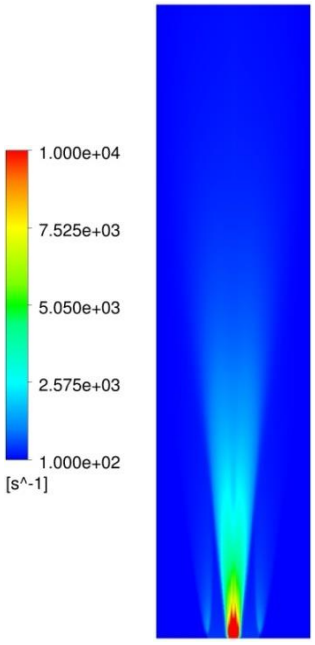

Figure 5.2. Turbulent Eddy frequency [Hz]

The thermo acoustic analysis is assessed on the study of the spray flame response at two different frequencies. The maximum and minimum forcing frequencies are chosen on the basis of the liquid phase characteristic times previously discussed. The inlet boundary condition is perturbed with a harmonic wave, represented by a cosine signal containing the forcing frequency. One case is run under an acoustic frequency of 1500 Hz, and the other one of 150 Hz. The oscillating time component of the velocity is implemented in the code, as follow:

$$u\,(t) = \bar{u}\ + u^I \cos(2\pi f t) \tag{7}$$

where $\bar{u}$ is the mean gas mixture velocity and u^I, corresponds to a constant amplitude of 8% of its mean value.

Fig.5.3 and 5.4 show the temperature profiles as a function of time, monitored in six axial locations, at a radial distance of $3mm$ from the centreline. In Fig. 5.3, oscillations in the temperature indicate the sensibility of the flame to acoustic wave. In the 1500 Hz case (Fig. 5.3b), the forcing is damped already at y = 250mm after an initial temperature jump of 1000K. Instead, further downstream (Fig. 5.4) the temperature field is affected by a small fraction of the acoustic cycle: no oscillations are present after an initial transient in both the 150 Hz and 1500 Hz case.

Fig. 5.5 shows an increase of the gas phase temperature closer to the nozzle; the change of the evaporation rate controls the burning rate and the flame becomes shorter. The first effect of the acoustic wave is to enhance the evaporation of the liquid phase, which as stated above, seems to control the combustion rate. These phenomena are equally present in both cases.

The flame response at 1500 Hz is shown in Fig. 5.6. The bigger droplets move away from the core zone of the spray, towards the pilot and slowing down in the cold air flow surrounding the flame. This suggests that the inertia play a crucial role in the spray-acoustics interaction. Bigger droplets have greater relaxation times, and once departed from their initial location, they do not follow the acoustic flow. Nevertheless, the radial dispersion of the droplets, Fig. 5.6 (c) is currently under further investigations. The behaviour of the smaller droplets can be partially investigated since the lower frequency response of the liquid is fixed by the evaporation time, and the maximum distance they reach is about x/D = 120mm. Nevertheless, when comparing it to the travel distance in the non-forced flame, one can deduce that the evaporation takes place quicker. Comparing Fig. 5.1b and Fig. 5.6b, the fuel mass fraction is higher in the forced flame, which indicates an higher evaporation rate.

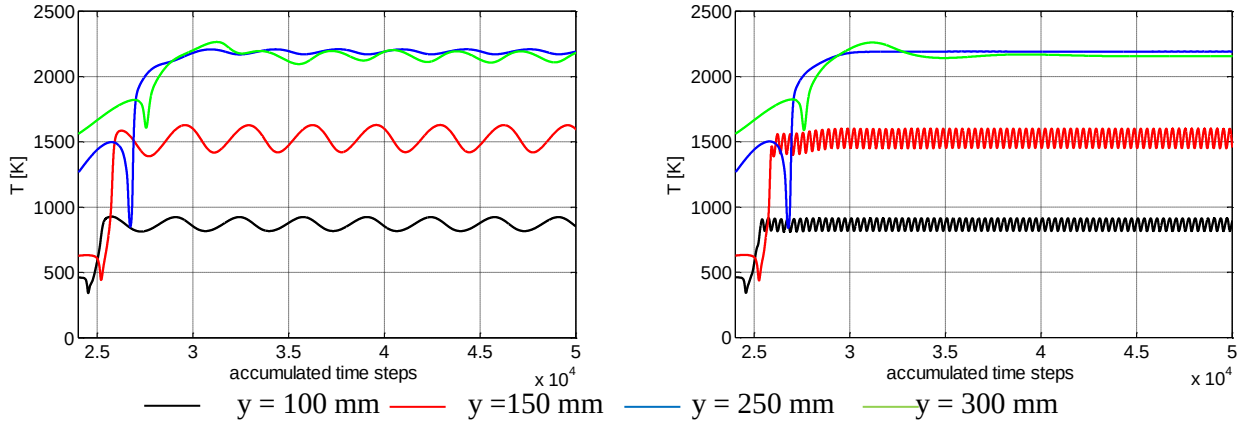

Figure 5.3. Instantaneous temperature: 150 Hz (left), 1500 Hz (right).

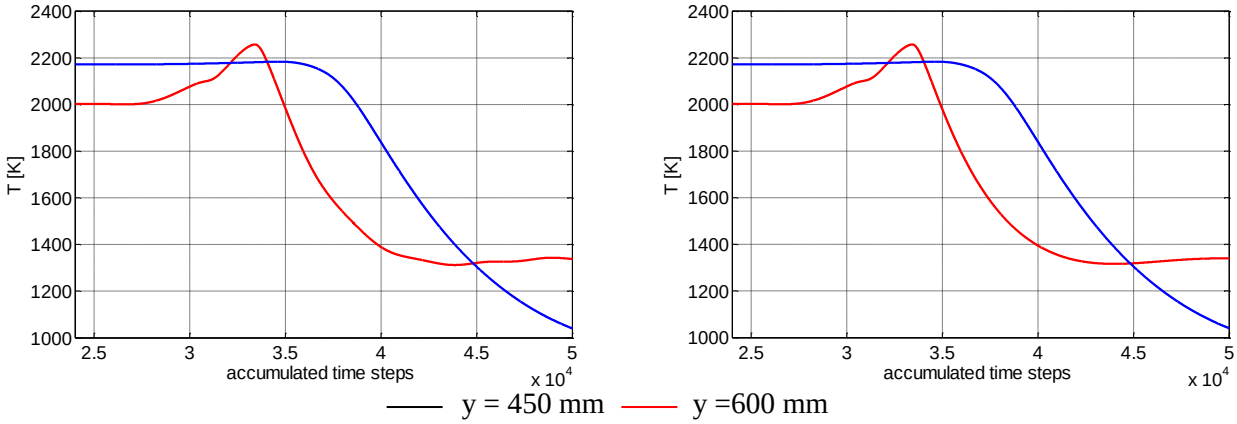

Figure 5.4. Instantaneous temperature: 150 Hz (left), 1500 Hz (right).

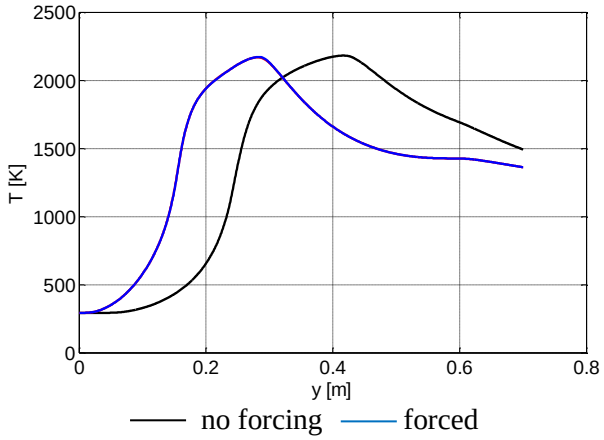

Figure 5.5. Time averaged temperature along the axial coordinate, x=3 mm.

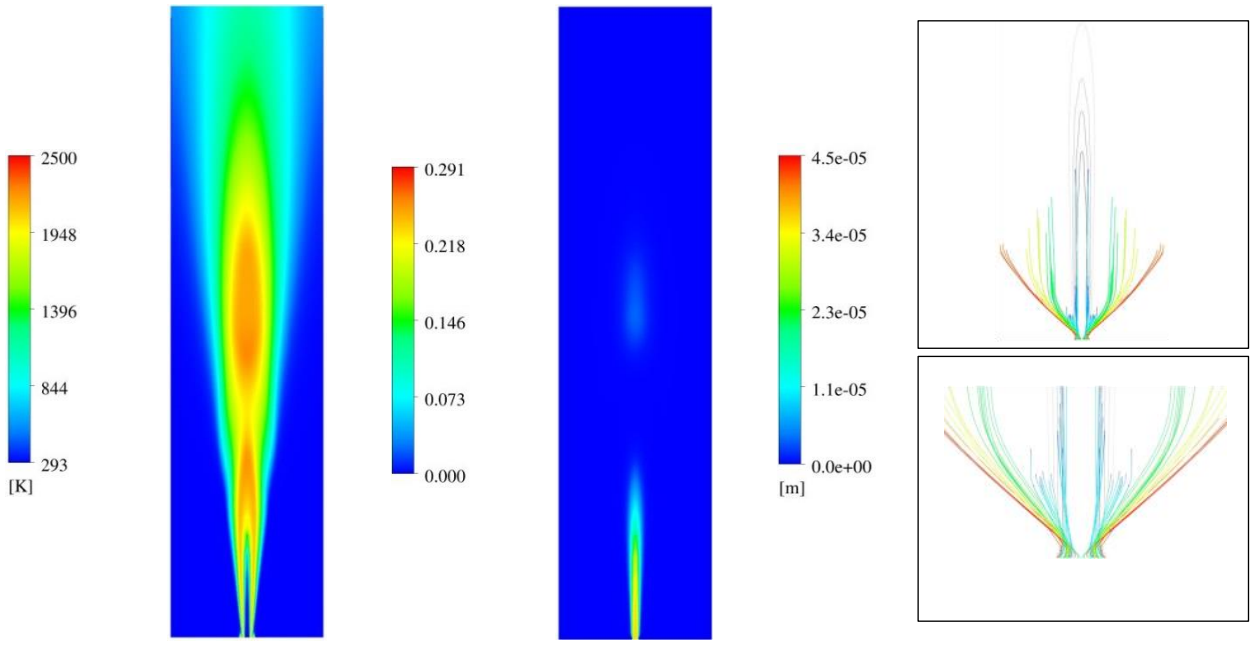

Figure 5.6. Instantaneous temperature (a), C_2H_6O mass fraction (b), liquid droplets diameter over gas fuel contours (grey lines) (c), at t=20ms. Acoustic forcing = 1500 Hz.

6. Conclusions

An effort has been made in this work, to capture the transient phenomena in a non confined spray flame. Under these conditions, the global flow field seems to be stable under acoustic forcing, even if at 150 Hz, the oscillations of the temperature are not damped downstream, as occurs at high frequency. Nevertheless, the dispersion of the droplets, at low and high frequency has to be investigated more carefully, in the case of a confined flame, where impingements on the walls are likely to take place. Same forcing frequencies have been imposed with two different amplitudes. The flame response does not change with the amplitude of the forcing frequency, at 1500 Hz, but shows larger temperature oscillations at 150 Hz, when the amplitude is increased from 8% to 12% of the mean velocity. The droplet lifetime seems to be affected by several parameters, such as droplets size class, radial and axial locations. Once again, this means that, the aerodynamic effects are dominant phenomena, and the local gas phase conditions can not be described entirely by the averaged flow field. A further refinement has to be done on the dispersed phase boundary conditions, in order to match the limit imposed by the computational cost with the need to increase the sampling size. Looking at the local liquid properties along the azimuthal direction, one can see that 3-D phenomena, especially under acoustic forcing, might be taken into account to understand the dynamics of the liquid response. Moreover, not a final statement can be formulated prior the implementation of the liquid turbulent dispersion, in the liquid-gas phase interaction.

REFERENCES

1. Gounder J. D., Kourmatzis A., Masri A. R. Turbulent piloted dilute spray flame: Flow fields and droplet dynamics. *Combustion and flame*, 159 (2012), 3372-3397.
2. Masri A. R, Gounder J. D . Details and complexities of boundary conditions in turbulent piloted dilute spray jets and flames, *Book chapter* 41-68.
3. Ansys CFX-Solver Modeling Guide, Version 14.0, (2011).
4. V. Fratalocchi, Internal report, University of Twente (2014).
5. L. Schiller and A. Naumann., *VDI Zeitz*, 77 p. 318, (1933).
6. W. E. Ranz & W. P. Marshall, Evaporation from drops, *Chem. Eng. Prog.*, Part 1, v. 48, 141–146 (1956).
7. M. M. El Wakil, O. A. Uyehara and P. S. Myers, A theoretical investigation of the heating up period of injected fuel droplets vaporising in air, NACA TN-3179 (1954).
8. P. Watkins and H. Khaleghi, Modelling diesel spray evaporation using a noniterative implicit solution scheme, *Appl. Math. Modelling*, 1990, Vol 14 (1990).
9. G. M. Faeth, Current status of droplet and liquid combustion, *Progress in Energy and Combustion Science*, vol. 3 pp 191-224 (1977).